Nikolay Dikoussar; Csaba Török
On one approach to local surface smoothing

Kybernetika, Vol. 43 (2007), No. 4, 533--546

Persistent URL: http://dml.cz/dmlcz/135795

KYBERNETIKA — VOLUME 43 (2007), NUMBER 4, PAGES 533 – 546

ON ONE APPROACH TO LOCAL SURFACE SMOOTHING

Nikolay Dikoussar and Csaba Török

A bicubic model for local smoothing of surfaces is constructed on the base of pivot points. Such an approach allows reducing the dimension of matrix of normal equations more than twice. The model enables to increase essentially the speed and stability of calculations. The algorithms, constructed by the aid of the offered model, can be used both in applications and the development of global methods for smoothing and approximation of surfaces.

Keywords: data smoothing, least squares and related methods, linear regression, approximation by polynomials, interpolation, computer aided design (modeling of curves and surfaces), surface approximation

AMS Subject Classification: 93E14, 93E24, 62J05, 41A10, 65D17, 65D05

1. INTRODUCTION

Methods of 3D data approximation and smoothing, and the related problems are of wide interest in theoretical and experimental sciences. The nature of dependence between the variables and the level of the accuracy of the measurements determine the tools and techniques the researchers can choose to treat data. To solve the complexity of the problem one can combine and modify different approaches.

The majority of existing techniques were developed from the corresponding techniques for 2D data with or without noise. The two main types of approximating polynomial surfaces are the rectangular tensor product surfaces [3] and the triangular patches [8]. When smoothing noisy data, on one side there are the nonparametric methods, such as kernel smoothers, wavelets and neural networks that do not result in functional equations [10, 12, 13], and on the other side the parametric ones, such as regression, interpolation and splines [2, 18], where e. g. the latter presents a fitting method, where local approximating polynomials on appropriate minimal segments are directly extended to splines. For a brief overview of the base approximating and smoothing methods see [9, 11].

The paper proposes a new approach to the task of local polynomial smoothing of surfaces of two variables by a bicubic model based on some pivot points of the surface. It considers a regression model for computing the estimate $\hat{F}_*$ of a smooth function $F(x, y)$ in a given point (x_*, y_*) using its measured points $\{\tilde{F}_k\}$ and special

basis functions. Papers [4, 5, 16, 15] considered algorithms that used pivot points for smoothing and approximation of one dimensional functions. The pivot (reference) points originate from the discrete projective transformation [5]. As fixed parameters of the model, they play a key role in the formulae. There are only two assumptions about them: they must be mutually different and form a rectangular grid. Different choice of pivot points can lead to models with different possibilities and properties.

It is well known that smoothing functions of two and more variables is characterized by enlarged complexity caused particularly by increasing the dimension of the matrix of the system of the normal equations. This complexity can be well demonstrated by comparing the interpolation of functions of one and two variables. It is well known too, that there are hardships with the polynomial regression models of order greater than 5 mainly for nets with equidistant step, where the matrix of the regression model is not well determined [1, 14].

We propose to use a cubic model for both variables for the local surface smoothing, in which one part (biquadratic) of the parameters is chosen on the surface as pivot points and the other part (bicubic) contains free parameters. Such a construction of a model enables to decrease the dimension of the matrix of the normal system more then two times.

The basis functions of the proposed bicubic model depend on the coordinates of 9 mesh points of a rectangle net and are expressed by one dimensional basis functions of a 3-point cubic spline, defined in [4]. This way we get an *incomplete bicubic polynomial model* (IBPM), in which the coefficient for x^3y^3 equals zero. The *pivot constrain* of this model results in a simplification of the numerical hardships connected with the solution to the normal system, when the approximating polynomial is of higher order [14], and in speeding up the computation almost three times. These qualitative characteristics seem to be valuable when using a model for solving practical problems, mainly in real time systems.

Qualitative algorithms for approximating and smoothing surfaces are necessary for many scientific and technical problems, when a complex functional dependence is replaced by a more simple (polynomial) one as in smoothing experimental data, partly in image processing, investigation of respond surfaces [14], analysis of magnetic structures etc. In [6] we suggested a new method to the analysis of complex 2D dependence. The proposed auto-tracking piecewise cubic approximation (APCA) divides the curve into segments of various lengths. In [17] we showed that APCA can be used to increase the wavelet compression rate. One of the main future tasks is to generalize APCA for global approximation of 3D data based on the IBPM model.

Section 2 is devoted to two cubic models with pivot constrains. The main incomplete bicubic model is constructed in Section 2.1. Section 2.2 introduces a full bicubic model. Section 3 demonstrates the qualitative properties of the IBPM in surface smoothing. Section 3.1 describes the regression procedure based on IBPM. The next section compares the numerical results of approximation of test functions by the new incomplete bicubic model and the corresponding classic model. The last section consists of conclusions.

2. BICUBIC MODEL WITH PIVOT CONSTRAIN

2.1. IBPM-model with nine pivot points

We consider a representation of a surface, where the rectangle domain $R : a \le x \le b;\ c \le y \le d$ is divided into rectangles $R_{ij} : x_{i-1} \le x \le x_i,\ y_{j-1} \le y \le y_j$ $(i = 1, 2, \ldots, N;\ j = 1, 2, \ldots, M)$. A surface $F(x, y)$ is defined on every such rectangle the way that it coincides with one of the four given curves $f_i(x),\ g_j(y)$ along the four sides of the rectangle R_{ij} [1].

We divide the R_{ij} into four parts by intervals parallel to the coordinate axes and construct a 9-point net (see Figure 1a), on which we will approximate the surface $F(x, y)$ with cubic functions $f_i(x),\ g_j(y)$.

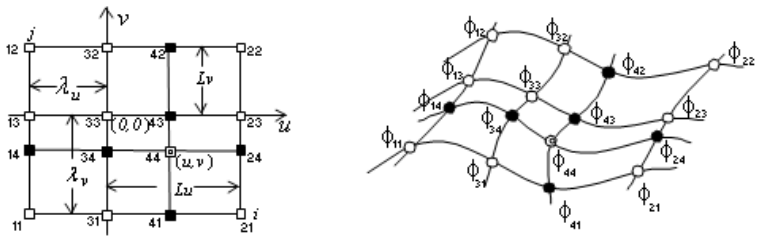

Fig. 1. The choice of mesh points and parameters of the net $\Delta_{\lambda L}$ (a) and the scheme of the construction of the approximant on the surface $z = \phi(u, v)$ (b).

Now we give a construction of a local approximation $C(u, v)$ of a function of two variables $F(x, y)$ on a 9-point net $\Delta_{\lambda L} = \Delta_{\Lambda_u} \times \Delta_{\Lambda_v}$ of the rectangle

$$R_{\lambda L} : \lambda_u \le u \le L_u,\ \lambda_v \le v \le L_v, \tag{1}$$

where $\Delta_{\Lambda_u} : \lambda_u = x_\lambda - x_0 < x_0 < x_L - x_0 = L_u,\ \Delta_{\Lambda_v} : \lambda_v = y_\lambda - y_0 < y_0 < y_L - y_0 = L_v,\ u = x - x_0, v = y - y_0$ and $x_\lambda, x_L,\ y_\lambda, y_L$ denote the edges of the rectangle.

We suppose that in the mesh points of a net $\Delta_{\lambda L}$ the values of the function are known $F_{ij} = F(x_i, y_j,),\ i \cdot j = 1, 2, 3$. For simplifying the formulae we shift the origin to the point $F(x_0, y_0)$ and introduce

$$\phi = F(x - x_0, y - y_0) - F(x_0, y_0) = \phi(u, v).$$

We denote the set of function values in mesh points by $\{\phi_{ij}\}$ (see Figure 1b), the parameters of the net by $\Lambda_{uv} : \{\Lambda_u; \Lambda_v\}, (\Lambda_u = [\lambda_u, L_u], \Lambda_v = [\lambda_v, L_v])$, and the full set of pivot points by $\mathcal{R}$ (mark).

Following [4] a local one dimensional three-point cubic spline of the variable τ can be constructed on the pivot points $\{\lambda_\tau, O, L_\tau\}, (\tau = u, v)$

$$S_3(\tau; \Lambda_\tau) = \sum_{i=1}^{3} f_i d_i(\tau; \Lambda_\tau) + \alpha Q(\tau; \Lambda_\tau), \tag{2}$$

where $\{f_i\}$ are the function values in the pivot points, $d_i(\tau;\Lambda_\tau)$ and $Q(\tau;\Lambda_\tau)$ are the basis functions and α is a free parameter. The basis functions are defined by the parameters of the set $\Delta_{\lambda L}$ as follows

$$\begin{aligned} d_1(\tau;\Lambda_\tau) &= -(\lambda_\tau H_\tau)^{-1}\tau(\tau - L_\tau), \\ d_2(\tau;\Lambda_\tau) &= (L_\tau H_\tau)^{-1}\tau(\tau - \lambda_\tau), \\ d_3(\tau;\Lambda_\tau) &= (\lambda_\tau L_\tau)^{-1}(\tau - \lambda_\tau)(\tau - L_\tau) \quad \text{and} \\ Q(\tau;\Lambda_\tau) &= \tau(\tau - \lambda_\tau)(\tau - L_\tau), \end{aligned} \tag{3}$$

where $H_\tau = L_\tau - \lambda_\tau (\tau = u, v)$. The basic parameters of the pivot rectangle, that defines the functions $d_i(\tau;\Lambda_\tau)$ and $Q(\tau;\Lambda_\tau)$, are shown in Figure 1a). The pivot points $\{\phi_{ij}\}$ of the surface in Figure 1.b) correspond to the mesh points $\Delta_{\lambda L}$.

We write the six cubic parabolas passing through three points of the set $\{\phi_{ij}\}$ along the six lines of the net $\Delta_{\lambda L}$ in the form

$$\begin{aligned} C_j(u;\mathcal{R}) &= \sum_{i=1}^{3} \phi_{ij} d_i(u;\Lambda_u) + \alpha_{uj} Q(u;\Lambda_u), \\ C_i(v;\mathcal{R}) &= \sum_{j=1}^{3} \phi_{ij} d_j(v;\Lambda_v) + \alpha_{vi} Q(v;\Lambda_v), \quad (i \cdot j = 1,2,3). \end{aligned} \tag{4}$$

In these equations the values ϕ_{ij} are fixed and the free coefficients α_{uj} and α_{vi} are unknown. The formulae in (4) can be used for computing $\phi(u,v)$ in any point (u,v) of the rectangle $R_{\lambda L}$: we choose one point (the fourth one, see ϕ_{14}, ϕ_{34}, ϕ_{24}, ϕ_{41}, ϕ_{43} and ϕ_{42} in Figure 1) on every curve and write the equation of the cubic parabola C_{4u} that passes through the corresponding three points and the actual one (u,v) in correspondence with (2) as

$$\begin{aligned} C_{4u} &= \sum_{i=1}^{3} C_i(v,\mathcal{R}) d_i(u;\Lambda_u) + \alpha_{u4} Q(u;\Lambda_u) \\ &= \sum_{i=1}^{3} [\sum_{j=1}^{3} \phi_{ij} d_j(v;\Lambda_v) + \alpha_{vi} Q(v;\Lambda_v)] d_i(u;\Lambda_u) + \alpha_{u4} Q(u;\Lambda_u) \\ &= \sum_{i=1}^{3}\sum_{j=1}^{3} \phi_{ij} w_{ij}(u,v;\Lambda_{uv}) + \sum_{k=1}^{3} \alpha_{vk} \omega_k(u,v;\Lambda_{uv}) + \alpha_{u4} Q(u;\Lambda_u) \\ &= S_q(u,v;\mathcal{R}) + \sum_{k=1}^{4} \alpha_{uk} \omega_k(u,v;\Lambda_{uv}), \end{aligned}$$

where

$$S_q(u,v;\mathcal{R}) = \sum_{i=1}^{3}\sum_{j=1}^{3} \phi_{ij} w_{ij}(u,v;\Lambda_{uv})$$

presents the biquadratic element C_{4u} with the basis functions

$$w_{ij}(u,v;\Lambda_{uv}) = d_i(u;\Lambda_u) d_j(v;\Lambda_v), \ (i \cdot j = 1,2,3),$$

and the bicubic element is presented by the convolution of the coefficients α_{uk} and the basis functions $\omega_k(u,v;\Lambda_{uv})$. An analogous formula can be written for the curve C_{4v} of variable v. Then we take for the approximation of $\phi(u,v)$ in the point (44) the average of these two functions and get

$$\phi_{44} \cong C(u,v;\mathcal{R}) = [C_{4u} + C_{4v}]/2 = S_q(u,v;\mathcal{R}) + \sum_{k=1}^{4} \frac{1}{2}(\alpha_{uk} + \alpha_{vk})\omega_k(u,v;\Lambda_{uv}),$$

where the basis functions $\omega_k(u,v;\Lambda_{uv})$ are expressed by the products

$$d_i(u;\Lambda_u)\,Q(v;\Lambda_v), \quad d_i(v;\Lambda_v)\,Q(u;\Lambda_u) \quad (i=1,2,3)$$

and the functions $Q(u;\Lambda_u),\ Q(v;\Lambda_v)$.

Taking into account the normalization property of the functions d_i and d_j ($d_3 = 1 - d_1 - d_2$), we get after some arrangements for $C(u,v;\mathcal{R})$

$$\begin{aligned} C(u,v;\mathcal{R}) &= \sum_{i\cdot j=1}^{3} \phi_{ij} w_{ij}(u,v;\Lambda_{uv}) + \sum_{m=1}^{6} \theta_m \omega_m(u,v;\Lambda_{uv}) \\ &= S_q(u,v;\mathcal{R}) + S_c(u,v;\Lambda_{uv}), \end{aligned} \tag{5}$$

where θ_m are the free coefficients. The functions $S_q(u,v;\mathcal{R})$ and $S_c(u,v;\Lambda_{uv})$ present the *biquadratic* and *bicubic* elements of $C(u,v;\mathcal{R})$, respectively. One can easily check that the surface (5) is a local bicubic spline over $\Delta_{\lambda L}$, for the functions and their derivatives are continuous in the mesh points.

Let us have a short look at the basic properties of the basis functions $w_{ij}(u,v;\Lambda_{uv})$ and $\omega_m(u,v;\Lambda_{uv})$. For $w_{ij}(u,v;\Lambda_{uv})$ we have

$$w_{ij}(i',j') = \delta_{ii'}\delta_{jj'} = \begin{cases} 1, \text{ if } & i = i' \text{ and } j = j', \\ 0, \text{ if } & i \neq i' \text{ and } j \neq j', \end{cases} \tag{6}$$

$$\sum_{i=1}^{3}\sum_{j=1}^{3} w_{ij}(u,v;\Lambda_{uv}) = 1, \tag{7}$$

since $\sum_{i=1}^{3} d_i(\tau;\Lambda_\tau) = 1$ ($\tau = u, v$) and so

$$\sum_{i=1}^{3}\sum_{j=1}^{3} w_{ij}(u,v;\Lambda_{uv}) = \sum_{i=1}^{3} d_i \left(\sum_{j=1}^{3} d_j\right) = 1 \sum_{i=1}^{3} d_i = 1 \cdot 1 = 1.$$

From (6) we get for one of the 9 points (i',j') of the net $\Delta_{\lambda L}$

$$s_q(i',j') = \sum_{i\cdot j} w_{ij}(i',j')\phi_{ij} = \sum_{i\cdot j} \delta_{ii'}\delta_{jj'}\phi_{ij} = \phi_{i'j'},$$

i. e. $S_q(u,v;\mathcal{R})$ coincides with $\phi(u,v)$ in every pivot point.

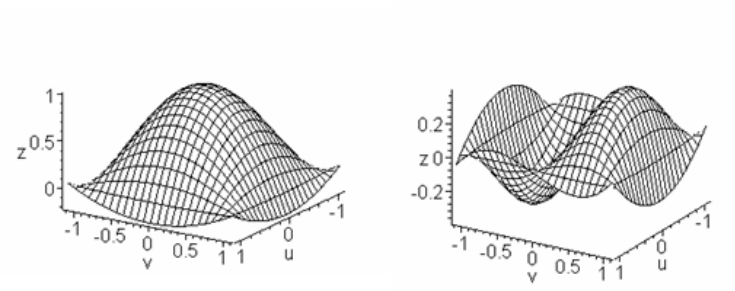

Fig. 2. The basis functions $w_{33}(u, v; \Lambda_{uv})$ and $\omega_4(u, v; \Lambda_{uv})$ for $\Lambda_{uv} : \{-1, 1; -1, 1\}$.

The basis functions $\omega(u, v; \Lambda_{uv})$, as it was mentioned above, are defined by $d_i(u; \Lambda_u)\, Q(v; \Lambda_v)$, $d_j(v; \Lambda_v)\, Q(u; \Lambda_u)$ $(i \cdot j = 1, 2)$, the functions $Q(u; \Lambda_u)$, $Q(v; \Lambda_v)$ and equal zero in the mesh points of $\Delta_{\lambda L}$, i. e.

$$\omega_m(u_i, v_j) = 0 \quad (m = 1, 2, \ldots 6;\ i \cdot j = 1, 2, 3).$$

The graphs in picture 2 correspond to two basis functions.

Since the element with the products u^3v^3 in the basis $C(u, v; \mathcal{R})$ is absent, the formula (5) presents an incomplete bicubic model of the surface, thus it corresponds to the classic polynomial model of two variables with fifteen coefficients and a basis

$$\{1, x, y, x^2, xy, y^2, xy^2, x^2y, x^3, y^3, xy^3, x^2y^2, x^3y, x^2y^3, x^3y^2\}. \tag{8}$$

The main feature of the IBPM construction is the fact, that nine of its parameters (the coefficients by w_{ij}) coincides with the values ϕ_{ij} of the considered surface and the other parameters (θ_m) are free.

If the values of the pivot coordinates are given without errors, then the number of unknown parameters in the model (5) is two and half times smaller (six instead of fifteen) than in the classic model of the bicubic interpolation spline (CBM) or *simple double cubic spline* with regards to the net $\Delta_{xy} = \Delta_x \times \Delta_y$ [1]:

$$s(x, y) = \sum_{\alpha=0}^{3} \sum_{\beta=0}^{3} a_{\alpha\beta} x^\alpha y^\beta, \quad x_{i-1} \le x \le x_i, \quad y_{j-1} \le y \le y_j. \tag{9}$$

The polynomial $s(x, y)$ interpolates the surface in the ijth cell of the net Δ_{xy} and depends on 16 free coefficients $a_{\alpha\beta}$. The use of the model (5) for local approximation of the function $F(x, y)$ is preferable to $s(x, y)$ in the case, when $\{\phi_{ij}\}$ are given with a higher precision and the pivot points lie in the mesh points of the rectangle net $\Delta_{\lambda L}$. These constrains are not very strong in practice. They can be achieved by an a priori choice of the mesh points of the pivot rectangle and by a more precise measurement (or by repeated measurements) of the pivot values. These requirements are the main limitation for the use of IBPM. Mention must be made that due to these constrains the effectiveness of the smoothing procedure increases essentially, for the

matrix dimension of the system of normal equations decreases more than twice. This raises the stability and the speed of the calculations. The model $C(u, v; \mathcal{R})$ from (5) serves for the polynomial approximation of $F(x, y)$ in the rectangle $R_{\lambda L}$ as a proper bicubic approximant, in which more than half of the coefficients (pivot points) may be computed a priori with a high precision based on the values of the polynomials $F(x, y)$ in the mesh points.

2.2. Full bicubic model (BM)

We construct over the rectangle net of 16 mesh points (all points in Figure 1a) a full bicubic model (BM) equivalent to (9), with a basis different from (8) and which is parameterized by the 16 pivot coordinates of the considered surface $z = F(x, y)$. We denote the net by $\Delta_{\lambda\mu\nu}$ and take in its mesh points the pivot points $\{\phi_{ij}\}$ $(i \cdot j = 1, \ldots, 4)$. The geometric sense of the parameters is shown in Figure 3.

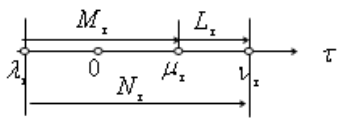

Fig. 3. The parameters of the net $\Delta_{\lambda\mu\nu}$ for $m_i(\tau; \Lambda_\tau)$ along of one axis.

We introduce the parameters $\lambda_\tau, \mu_\tau, \nu_\tau$ and construct four functions on the base of Lagrange cubic interpolation polynomial in the form

$$\begin{aligned} m_1(\tau; \Lambda_\tau) &= (\lambda_\tau N_\tau M_\tau)^{-1} \tau(\tau - \mu_\tau)(\tau - \nu_\tau), \\ m_2(\tau; \Lambda_\tau) &= -(\mu_\tau M_\tau L_\tau)^{-1} \tau(\tau - \lambda_\tau)(\tau - \nu_\tau), \\ m_3(\tau; \Lambda_\tau) &= (\nu_\tau L_\tau N_\tau)^{-1} \tau(\tau - \lambda_\tau)(\tau - \mu_\tau), \\ m_4(\tau; \Lambda_\tau) &= -(\lambda_\tau \mu_\tau \nu_\tau)^{-1} (\tau - \lambda_\tau)(\tau - \nu_\tau)(\tau - \mu_\tau), \end{aligned} \tag{10}$$

where $L_\tau = \nu_\tau - \mu_\tau$, $M_\tau = \mu_\tau - \lambda_\tau, N_\tau = \nu_\tau - \lambda_\tau, (\tau = u, \nu)$ and Λ_τ denotes the set of numbers $\Lambda_\tau \equiv \{\lambda_\tau, \mu_\tau, \nu_\tau, L_\tau, M_\tau, N_\tau\}$.

We define by the analogy with IBPM the basis functions w_{ij} as products $w_{ij}(u, v; \Lambda_{uv}) = m_i(u; \Lambda_u) m_j(v; \Lambda_v)$. Then the full bicubic model may be written as

$$C_{BM} = \sum_{i=1}^{4} \sum_{j=1}^{4} \phi_{ij} w_{ij}(u, v; \Lambda_{uv}), \tag{11}$$

where $\Lambda_{uv} = \{\Lambda_u, \Lambda_v\}$ denotes the parameters of the net $\Delta_{\lambda\mu\nu}$.

One can easily check by the analogy with the 9 point set that the basis functions $w_{ij}(u, v; \Lambda_{uv})$ have the properties (6) and (7).

When the values $\{\phi_{ij}\}(i \cdot j = 1, \ldots, 4)$ are given precisely the model (11) is an interpolant of polynomial (9). When the pivot points $\{\tilde{\phi}_k\}$, $k = 1, 2, \ldots, N$ $(N \gg 16)$ are unknown the BM for smoothing the parts of the surface on the base of observed points $\{\tilde{\phi}_{ij}\}$ is more stable than the classic model (9), since the determinant of the normal system *gets better* by several orders and the computation of estimates $\{\hat{\phi}_k\}$ gets more stable (see Section 3.2).

3. BICUBIC SURFACE SMOOTHING

The least square procedure is considered in this section on the base of IBPM for local smoothing (approximation) of surfaces with bicubic polynomials in a region given by a rectangle $R_{\lambda L}$. The quality of processing the same samples by the model $C(u, v; \mathcal{R})$ and $s(x, y)$ are compared on the base of numerical results when $a_{33} = 0$.

3.1. Regression procedure with IBPM

We consider the task of smoothing the measured points $\{\tilde{F}_k\},\ k = 1, 2, \ldots, n$ ($n \gg 15$) of the surface $z = F(x, y)$ on the base of model (5). For this the sample $\{\tilde{F}_k\}$ has to contain besides the measurements nine pivot points $\{\tilde{F}_{ij} = F_{ij} + e_{ij}\}$ ($e_{ij} \sim N(0, \sigma_e^2),\ i \cdot j = 1, 2, 3,$) that lie around the basis point $(0, 0, \tilde{F}_0)$ in the mesh points of a rectangle net $\Delta_{\lambda L}$ (1). We define $w_{ij}(x, y; \Lambda_{xy})$, $\omega_m(x, y; \Lambda_{xy})$ on the basis of parameters Λ_{xy} and build the *pivot surface* $\tilde{S}_q(x, y; \mathcal{R})$ in the form

$$\tilde{S}_q(x, y; \mathcal{R}) = \sum_{i=1}^{3}\sum_{j=1}^{3} \tilde{F}_{ij} w_{ij}(x, y; \Lambda_{xy}) = \sum_{i=1}^{3}\sum_{j=1}^{3} (F_{ij} + e_{ij}) w_{ij}(x, y; \Lambda_{xy}). \qquad (12)$$

Let $\tilde{\boldsymbol{Z}}^T = [\tilde{F}_1 - \tilde{S}_{q1}, \ldots, \tilde{F}_n - \tilde{S}_{qn}]$ be a vector gained by subtracting from the observations $\tilde{F}_1, \tilde{F}_2, \ldots, \tilde{F}_n$ the values $\tilde{S}_{qk}$, computed by the formula (12) with pivot points $\{\tilde{F}_{ij}\}$ and values $\{w_{ijk}\}$. Then $\tilde{\boldsymbol{Z}} = \boldsymbol{Z} + \boldsymbol{e}_{\mathcal{R}} + \boldsymbol{e}_F$, where $\boldsymbol{e}_F$ is the error vector of the sample $\{\tilde{F}_k\}$ and the vector $\boldsymbol{e}_{\mathcal{R}}^T = [e_{r1}, e_{r2}, \ldots, e_{rm}]$ is generated by the convolution of errors $\{e_{ij}\}$ of the pivot points and the values of the basis functions $\{w_{ijk} = w_{ij}(x_k, y_k)\},\ k = 1, 2, \ldots, n$.

Let us examine the characters of the errors $\boldsymbol{e}_{\mathcal{R}}$ in more detail. Since $\sum_{ij} w_{ij} = 1$, based on (12) and the properties of w_{ij} we get $|e_{\mathcal{R}k}| \le e_{r\max}$ ($e_{r\max} = \max_{ij}\{|e_{ij}|\}$). Additionally if the parameters Λ_{xy} are chosen symmetrically with respect to the basis point (x_0, y_0), then for $x,\ y \in R_{\lambda L}$: $0.4 \le \sum_{ijk} w_{ijk}^2 \le 1$. Therefore the variance of $e_{\mathcal{R}}$ will not be greater than σ_e^2 (the experimental estimation is $\sigma_{\mathcal{R}}^2 \approx \frac{1}{2}\sigma_e^2$.)

We consider the smoothing process of the sample $\{\tilde{F}_k\},\ k = 1, 2, \ldots, n$, on the base of (5) in the form

$$Z \equiv F - S_q = (\Theta, \boldsymbol{B}) + e, \qquad (13)$$

where $\Theta^T = [\theta_0, \theta_1, \ldots, \theta_6]$ - the vector of unknown parameters, $\boldsymbol{B}^T = [1, \omega_1, \ldots, \omega_6]$ – the basis vector and e – the error. On the base of n ($n \gg 15$) measurements on the surface within the rectangle $R_{\lambda L}$ we get the vector $\tilde{\boldsymbol{Z}}$, compute for every measured point the basis functions $\omega_{mk} = \omega_m(x_k, y_k; \Lambda_{xy})$, construct the vectors $[1, \omega_{m1}, \omega_{m2}, \ldots, \omega_{mn}]^T$ and form the regression matrix $\Omega_{n \times n_p}$ with elements ω_{mk}, where $k = 1, 2, \ldots, n$; $m = 1, 2, \ldots, n_p - 1$. The rank of the matrix is n_p ($n_p = 7$) due to the linear independence of $\omega_m,\ m = 0, \ldots, 6$. We get a system of n equations

$$\boldsymbol{Z} = \Omega\Theta + \boldsymbol{e}$$

and use the LS criterion for getting the optimal estimator

$$\sum_{k=1}^{n} e_k^2 \to \min_{\Theta},$$

that enables to write the solution in the form

$$\hat{\Theta} = (\Omega^T \Omega)^{-1} \Omega^T \tilde{\boldsymbol{Z}}. \tag{14}$$

3.2. Numerical experiments

Example 1. We chose a fragment (see Figure 4) on the function Franke (see Matlab 5)

$$\begin{aligned} \Phi(x,y) \quad = \quad & 0.75e^{(-(9x-2)^2-(9y-2)^2)/4} + 0.75e^{(-(9x+1)^2/49-(9y+1)^2/10)} \\ & + 0.5e^{(-(9x-7)^2-(9y-3)^2)/4} - 0.2e^{(-(9x-4)^2-(9y-7)^2)} \end{aligned} \tag{15}$$

for setting working characteristics of the smoothing process by the IBPM in the form(13) and for their comparing with the working characteristics of the classic model (CBM) (9). We generated a sample $\tilde{F}_k = \{F(x_k, y_k) + e_k\}, k = 1, 2, \ldots, n$ ($n = 100, \sigma_e^2 = .01$) in the rectangle $R_{\lambda L}$ with parameters $x_0 = 0.62, y_0 - 0.2; \lambda_x = -0.15, L_x = 0.25; \lambda_y = -0.25, L_y = 0.25$ and chose the coordinates of the pivot points $\{\tilde{F}_{ij} = F_{ij} + e_{ij}\}$ with the same parameters but different errors.

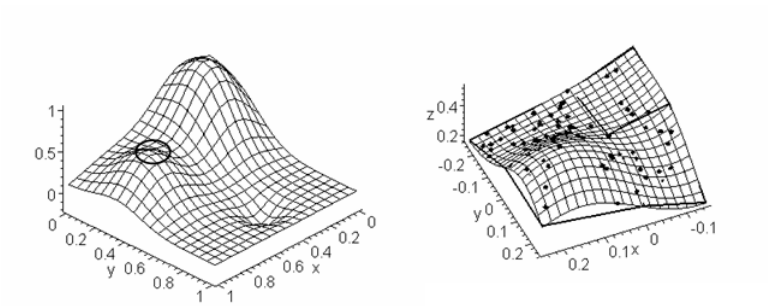

Fig. 4. The surface $\Phi(x, y)$ and its fragment on the net $\Delta\Lambda L$ with points $\{\tilde{F}_k\}$.

The result of smoothing by IBPM were compared with the results of processing the same samples by the CBM (9) with 15 parameters. The following characteristics were computed for both models:

a) maximal bias $r_{\max} = \max_{x,\, y \in R_{\lambda L}} |F - \hat{F}|$;

b) the determinant of the matrix of the normal equations $det = \det(\Omega^T \Omega)$;

c) the global relative error r_e

$$r_e = \sqrt{\sum_{k=1}^{n} (\tilde{F}_k - \hat{F}_k)^2} \Big/ \sqrt{\sum_{k=1}^{n} \tilde{F}_k^2};$$

d) the time t_R, needed for computation $\hat{\Theta}$ and $\{\hat{F}_k\}$;

e) the distribution of residuals r_k

$$r_k = \tilde{F}_k - (\tilde{S}_{qk} + \hat{S}_{ck}), \quad \text{where} \quad \hat{S}_{ck} = \sum_{m=0}^{6} \hat{\theta}_m \omega_m(x_k, y_k), \quad m = 0, \ldots, 6.$$

The results of computations are in Figures 5, 6 and Table 1.

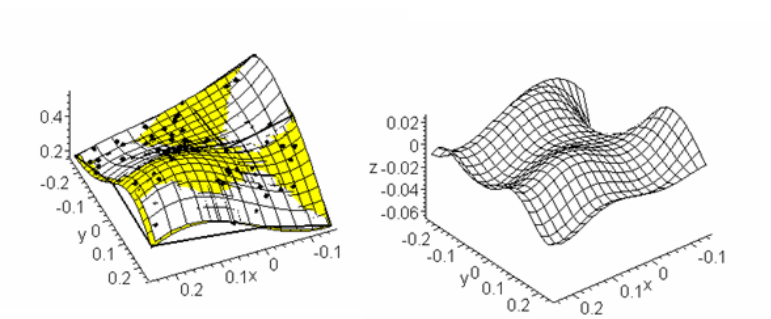

Fig. 5. The generated points (measurements) with the original and smoothed fragments of the surface (left) and their difference (right) $F(x, y) - \hat{F}(x, y),\ x,\ y \in R_{\lambda L}$.

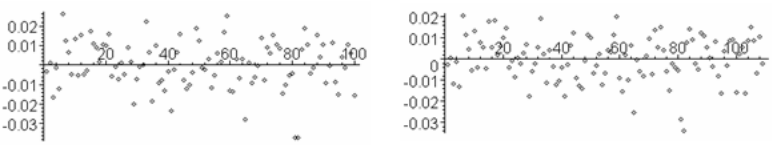

Fig. 6. The plots of residuals r_k for IBPM (left) and CBM (right).

The IBPM polynomial estimation of $\Phi(x, y)$ in the rectangle $R_{\lambda L}$ after rearrange-

Table 1. Computational characteristics of IBPM and CBM.

p_{model}	$p_{C(u,v;\mathcal{R})}$	$p_{s(x,y)}$	p_s/p_C
$r_{\max}$	0.027634635	0.065944316	2.386
r_e	0.032342485	0.030555841	0.94476
t_R	1.999	6.046	3.024
det	$0.1124\ 10^{-20}$	$0.2741\ 10^{-45}$	$2.4\ 10^{-25}$

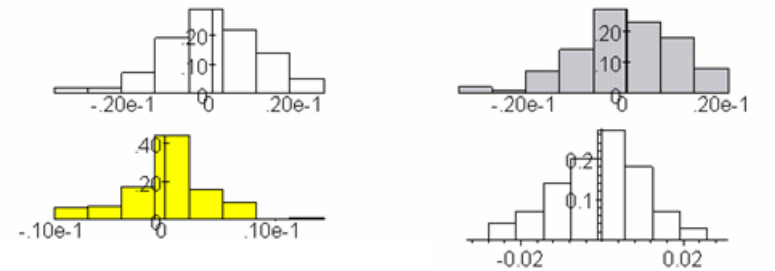

Fig. 7. The histograms of residuals r_k (top), their differences (left bottom) and the generated input errors (right bottom).

ments equals

$$\begin{aligned}\hat{F}(x,y) &= .4175140769x + .3960975192y + 153.7570490x^3y^2\\ &+ 201.5982904x^2y^3 - 15.47776507x^2y - 2.357156253xy^2\\ &- 21.61381719x^3 - 7.664238316y^3 - 31.29530791x^2y^2\\ &+ 7.819547029xy - 18.19242050x^3y - 68.64178532xy^3\\ &+ 3.374577403x^2 - 1.424124687y^2 + .3811368802.\end{aligned}$$

Example 2. Table 2 and Figures 8 – 11 contain the results of smoothing the sphere

$$F(x,y) = \sqrt{4-(x-1)^2-(y-1)^2}, \quad x,\, y \in [-1,1;-1,1]$$

with the net parameters $x_0 = 1,\ y_0 = 1;\ \lambda_x = -1,\ L_x = 1; \lambda_y = -1,\ L_y = 1$ for IBPM and CBM ($n = 150,\ \sigma_e^2 = .03$).

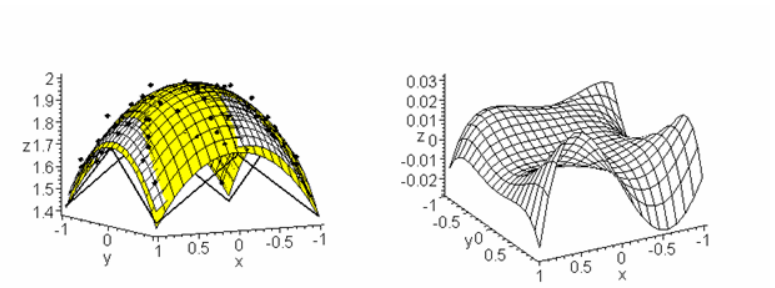

Fig. 8. The generated points (measurements) with the original and smoothed fragments of the sphere (left) and their difference (right) $F(x,y) - \hat{F}(x,y),\ x,\, y \in R_{\lambda L}$ (IBPM).

The IBPM estimation after rearrangement is given by

$$\begin{aligned}\hat{F}(x,y) &= -.03073090818xy^3 - .009867930550xy + .03826875230x^2y^3\\ &- .03152597740x^2y - .001729060898x^3 + .003677417398x\\ &+ .03811583823x^3y + .06483166127x^3y^2 - .05410740427xy^2\\ &- .003670835986y^3 + .006565254986y + 2.000586591\\ &- .2724256710y^2 - .04084875440x^2y^2 - .2603127485x^2.\end{aligned}$$

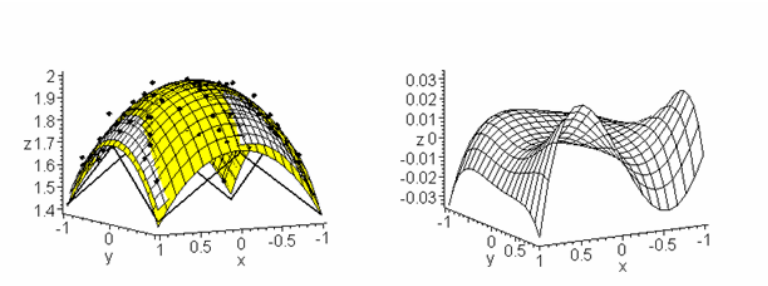

Fig. 9. The generated points with the original and smoothed fragments of the sphere (left) and their difference (right) (CBM).

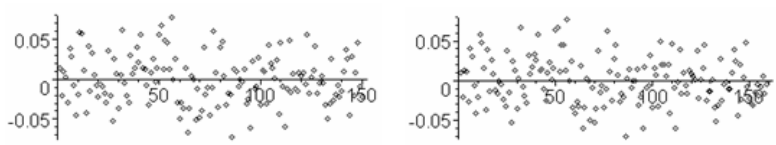

Fig. 10. The plots of residuals r_k for IBPM (left) and CBM (right).

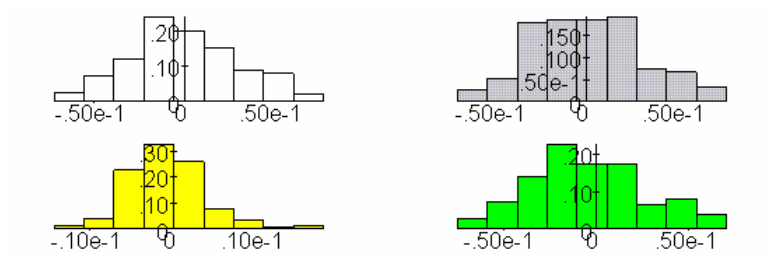

Fig. 11. The histograms of residuals r_k (top), their differences (left bottom) and the generated inputs errors (right bottom).

Table 2. Computational characteristics of sphere smoothing.

p_{model}	$p_{C(u,v;\mathcal{R})}$	$p_{s(x,y)}$	p_s/p_C
$r_{\max}$	0.03377820628	0.042366500	1.254255470
r_e	0.01662175319	0.016726239	1.006286103
t_R	3.180	9.205	2.89465
det	$0.76193\ 10^4$	$0.11439\ 10^{13}$	$0.1501319\ 10^9$

We can conclude on the base of the quality of the residuals (Figures 6, 7, 10, 11) and the numerical characteristics (Tables 1, 2) that the polynomial IBPM estimators (16), (17) are adequate and may be used for the approximation of the surfaces in $R_{\lambda L}$.

4. SOME REMARKS ON GLOBAL APPROXIMATION

Let us have a look at how to create global piecewise approximation based on the local IBPM model presented above, as we see it today. Once one has an effective local approximating tool, in global piecewise approximation the two principal tasks are to get the appropriate number of segments and ensure their continuity. In solving it every approach has its own pros and cons. In our case the benefits seem to be the simplicity of the model, the speed and stability of the computation. The concerns are the accuracy of the pivot points and the rectangle structure of their positions.

To use IBPM for global approximation we see several directions. The first naive approach can leverage the base property of the model: selecting the pivot points on the boundary of the neighbor local segments, the approximants will be continuous in the pivot points.

In [6] we suggested a new global method for the analysis of complex 2D dependence with relatively small errors. The proposed auto-tracking piecewise cubic approximation (APCA) divides the interval/curve into subintervals/segments of various lengths, provides local cubic estimations for every segment (stage 1) and gives a technique for obtaining integral cubic approximants (stage 2). Finding the breakpoints, knots in an autotracking mode and the iterative computation schemes are the two main features of the proposed method that uses an approximation model that is the 2D counterpart of IBPM. One of the main tasks is to generalize APCA for approximation of 3D data with surfaces. The main idea is clear: using 2D APCA in both directions (x and y) by partitioning create rectangles, and construct local surfaces over them. The paper [7] showed that this approach in combination with splines works efficiently on real noisy data too.

5. CONCLUSIONS

The results presented above show that the proposed new approach to the construction of (an incomplete) bicubic model for the local surface approximation by pivot points enables to raise the speed and stability of computations and reduce the dimension of the matrix of the normal system more then two times. The qualitative characteristics of the model suggest that the IBPM can serve as a basic construction for algorithms in global approximation and smoothing surfaces.

One of the main challenges is to generalize the presented IBPM model and APCA for global approximation of 3D data with surfaces.

ACKNOWLEDGEMENT

This work was partially supported by VEGA Grant 1/1006/04 MŠ.

(Received March 5, 2006.)

REFERENCES

[1] J. H. Ahlberg, E. N. Nilson, and J. L.Walsh: The Theory of Splines and Their Applications. Academic Press, New York 1967.
[2] O. Davydov and F. Zeilfelder: Scattered data fitting by direct extension of local polynomials with bivariate splines. Adv. Comp. Math. *21* (2004), 223–271.
[3] C. de Boor: Bicubic spline interpolation. J. Math. Phys. *41* (1962), 212–218.
[4] N. D. Dikoussar: Function parametrization by using 4-point transforms. Comput. Phys. Comm. *99* (1997), 235–254.
[5] N. D. Dikoussar: Adaptive projective filters for track finding. Comput. Phys. Comm. *79* (1994), 39–51.
[6] N. D. Dikoussar and Cs. Török: Automatic knot finding for piecewise-cubic approximation. Math. Model. *T-18* (2006), 3, 23–40.
[7] N. D. Dikoussar and Cs.Török: Data smoothing by splines and free knots. In: Proc. MMCP 2006 (in print)
[8] G. E. Farin: Triangular Bernstein–Bezier patches. Comput. Aided Geom. Design *3* (1986), 2, 83–127.
[9] G. Farin: History of curves and surfaces in CAGD. In: Handbook of CAGD (G. Farin, M. S. Kim and J. Hoschek, eds.), North Holland, Amsterdam 2002.
[10] W. Härdle: Applied Nonparametric Regression. Cambridge University Press, Cambridge 1990.
[11] C. Loader: Smoothing: Local regression techniques In: Handbook of Computational Statistics (J. E. Gentle et al., eds.), Springer–Verlag, Berlin 2004.
[12] S. Mallat: A Wavelet Tour of Signal Processing. Academic Press, New York 1999.
[13] B. D. Riplay: Pattern Recognition and Neural Networks. Cambridge University Press, Cambridge 1996.
[14] G. A. Seber: Linear Regression Analysis. Wiley, New York 1977.
[15] Cs. Török: 4-point transforms and approximation. Comput. Phys. Comm. *125* (2000), 154–166.
[16] Cs. Török and N. D. Dikoussar: Approximation with discrete projective transformation. Comput. Math. Appl. *38* (1999), 211–220.
[17] Cs. Török and T. Kepič: Data compression based on auto-tracking piecewise cubic approximation and wavelets. In: SICAM Plovdiv 2005, p. 274.
[18] G. Wahba: Spline Models for Observational Data. SIAM, Philadelphia 1990.

Nikolay Dikoussar, Joint Institute for Nuclear Research, Dubna. Russia.
e-mail: dnd@jinr.ru

Csaba Török, Department of Mathematics, Technical University of Košice, Vysokoškolská 4, 042 00 Košice. Slovak Republic.
e-mail: csaba.torok2@gmail.com